cases the plate buckles for voltages considerably lower than the breakdown voltage limits. The relative values of the displacements presented in Fig. 1 show that the plate loses stability according to different modes whether there are tensile or compressive in-plane piezoelectric stresses. Of course, larger values of v_0 are needed to buckle the plate for larger values of thickness. Considering that the voltage applied to the actuator is limited to the breakdown voltage, the effect of stress stiffening is more pronounced for thin plates.

Figure 2 shows that the configuration with the piezoelectric elements forming a frame around the perimeter of the plate presents a behavior similar to that of the plate with two longitudinal actuators along the edges (Fig. 1), but the stress-stiffening effect is more pronounced. For compressive in-plane piezoelectric actuation, the plate stiffness decreases until it loses stability for a relatively low voltage (about −70 V). Tensile actuation initially causes the plate stiffness to increase, but the plate loses stability according to a different mode at an actuation voltage of about 100 V.

V. Conclusion

The numerical results on the shape control of laminated plates with piezoelectric actuators demonstrate that even if the plate is unconstrained the piezoelectrically induced in-plane stresses may significantly affect the mechanical behavior of the plate. Therefore, for the case of combined in-phase and out-of-phase piezoelectric actuation, accurate modeling of composite plates with piezoelectric elements should account for the stress-stiffening effects. The importance of the stress-stiffness effect depends on the magnitude of the in-phase actuation and geometric arrangement of the piezoelectric actuators, boundary conditions, geometry of the problem, and material properties.

The ability of controlling the plate stiffness has potentially interesting applications in smart structures. For example, piezoelectric actuation systems may be designed to tune the vibration frequencies of composite plates. Also, the problem of buckling control of composite plates with piezoelectric elements can be properly modeled using the present formulation.

Acknowledgment

The author acknowledges CNPq (Brazilian National Research Council) for the financial support received for this work under Grant 300219/90-3.

References

[1]Crawley, E. F., and Anderson, E. H., "Detailed Models of Piezoceramic Actuation of Beams," *Journal of Intelligent Material Systems and Structures*, Vol. 1, No. 1, 1990, pp. 4–25.

[2]Crawley, E. F., and de Luis, J., "Use of the Piezoelectric Actuators as Elements of Intelligent Structures," *AIAA Journal*, Vol. 25, No. 10, 1987, pp. 1373–1385.

[3]Ha, S. K., Keilers, C., and Chang, F.-K., "Finite Element Analysis of Composite Structures Containing Distributed Piezoceramic Sensors and Actuators," *AIAA Journal*, Vol. 30, No. 3, 1992, pp. 772–780.

[4]Batra, R. C., Liang, X. Q., and Yang, J. S., "Shape Control of Vibrating Simply Supported Rectangular Plates," *AIAA Journal*, Vol. 34, No. 1, 1996, pp. 116–122.

[5]Tzou, H. S., and Ye, R., "Analysis of Piezoelastic Structures with Laminated Piezoelectric Triangle Shell Elements," *AIAA Journal*, Vol. 34, No. 1, 1996, pp. 110–115.

[6]Chandra, R., and Chopra, I., "Structural Modeling of Composite Beams with Induced-Strain Actuators," *AIAA Journal*, Vol. 31, No. 9, 1993, pp. 1692–1701.

[7]Yang, I. H., and Shieh, J. A., "Vibrations of Initially Stressed Thick Rectangular Orthotropic Plates," *Journal of Sound and Vibration*, Vol. 119, No. 3, 1987, pp. 545–558.

[8]Almeida, S. F. M., and Hansen, J. S., "Enhanced Elastic Buckling Loads of Composite Plates with Tailored Thermal Residual Stresses," *Journal of Applied Mechanics*, Vol. 64, No. 4, 1997, pp. 772–780.

[9]Rammerstorfer, F. G., "Increase of the First Natural Frequency and Buckling Load of Plates by Optimal Fields of Initial Stresses," *Acta Mechanica*, Vol. 27, No. 1–4, 1977, pp. 217–238.

[10]Heppler, G. R., and Hansen, J. S., "A Mindlin Element for Thick and Deep Shells," *Computer Methods in Applied Mechanics and Engineering*, Vol. 54, No. 1, 1986, pp. 21–47.

[11]Oguamanam, D. C. D., Almeida, S. F. M., and Hansen, J. S., "Stress Stiffening Effects in Laminated Beams with Piezoelectric Actuators," *Journal of Intelligent Material Systems and Structures*, Vol. 9, No. 2, 1999, pp. 137–145.

A. Chattopadhyay
Associate Editor

Coevolutionary Approaches to Structural Optimization

Min-Jea Tahk*
Korea Advanced Institute of Science and Technology, Taejon 305-701, Republic of Korea
Youdan Kim†
Seoul National University, Seoul 151-742, Republic of Korea
and
Changho Nam‡
Hankook Aviation University, Kyonggi 412-791, Republic of Korea

Introduction

NONGRADIENT methods such as genetic algorithms have been applied to solve structural optimization problems with promising results.[1–4] Nonetheless, these evolutionary algorithms have not been fully developed to handle constrained optimization.[5] Until recently, all existing methods were based on the evolution of a single group. Based on the evolution of two groups with opposite objectives, a coevolution method has been devised for solving saddle-point problems.[6] This method finds two major application areas: min/max design and constrained optimization. For a constrained problem, the optimal values of the parameter and multiplier vectors correspond to the saddle point of the associated Lagrangian if a certain convexity assumption is satisfied. Hence, constrained optimization problems can be reformulated as saddle-point problems. For nonconvex problems, augmentation of the Lagrangian function provides the necessary convexity, as with the deterministic augmented Lagrangian methods. The new coevolution method has been applied to the well-known truss problems: the 10-bar, 25-bar, and 72-bar truss problems treated in Refs. 7 and 8. The numerical results clearly show that the coevolution method has good potential for large-scale structural optimization. The basic concept of the coevolution method and its application to the 72-bar truss problem are summarized here.

Coevolution for Constrained Optimization

A general constrained optimization problem is written as follows:

$$\min_x f(x), \qquad x \in \mathcal{S} \tag{1}$$

subject to

$$g_i(x) \le 0, \qquad i = 1, \ldots, m \tag{2}$$

$$h_j(x) = 0, \qquad j = 1, \ldots, l \tag{3}$$

Received 6 October 1998; revision received 25 March 1999; accepted for publication 25 March 1999.

*Associate Professor, Department of Aerospace Engineering, 373-1 Kusong Yusong. Senior Member AIAA.

†Associate Professor, Department of Aerospace Engineering. Senior Member AIAA.

‡Associate Professor, Department of Aeronautical and Mechanical Engineering, Koyang. Senior Member AIAA.

where $\mathcal{S}$ is the search space of x. From now on, vector notations such as $g(x) \le 0$ and $h(x) = 0$ will be used for simplicity. The Lagrangian function for the primal problem is given by

$$L(x, \mu, \lambda) = f(x) + \mu^T g(x) + \lambda^T h(x) \tag{4}$$

where μ is a $m \times 1$ multiplier, and λ is an $l \times 1$ multiplier. It is well known that the triplet (x^*, μ^*, λ^*) satisfying the Kuhn–Tucker conditions is a saddle point of $L(x, \mu, \lambda)$ if the primal problem is convex over $\mathcal{S}$; $f(x)$ and $g(x)$ are convex and $h(x)$ is affine over $\mathcal{S}$ (Ref. 9). The saddle-point solution satisfies

$$L(x^*, \mu, \lambda) \le L(x^*, \mu^*, \lambda^*) \le L(x, \mu^*, \lambda^*) \tag{5}$$

for all $x \in \mathcal{S}$ and $\mu \ge 0$.

For nonconvex problems, we rely on an augmented Lagrangian function $L_A(x, \mu, \lambda, \rho)$ that includes penalty terms associated with the constraints to have an unconstrained local minimum at x^* for $\mu = \mu^*$ and $\lambda = \lambda^*$. The common practice of classical augmented Lagrangian methods is to employ quadratic penalty terms of the form

$$L_A(x, \mu, \lambda, \rho) = f(x) + \sum_{i=1}^{m} p_i(x, \mu_i, \rho) + \lambda^T h(x) + \rho h(x)^T h(x) \tag{6}$$

As discussed in Ref. 9, the penalty term p_i for the ith inequality constraint is calculated as

$$p_i(x, \mu_i, \rho) = \begin{cases} \mu_i g_i(x) + \rho g_i^2(x) & \text{if} \quad g_i(x) \ge -\mu_i/2\rho \\ -\mu_i^2/4\rho & \text{if} \quad g_i(x) < -\mu_i/2\rho \end{cases} \tag{7}$$

The advantages of the augmented Lagrangian formulation are twofold: A constrained problem is transformed into an unconstrained one, and the exact solution can be achieved. The latter is not true for simple penalty function methods.

The saddle-point problem can be interpreted as a zero-sum static game played by the parameter vector x and the multipliers μ, λ. In the coevolution approach, the zero-sum game is approximated by a matrix game, which is solved and updated at each generation. In the following, key features of the coevolution method are described.

Consider a zero-sum game for which a payoff function $F = F(u, v)$ is to be minimized by $u \in U$ and maximized by $v \in V$. It is assumed that $F = F(u, v)$ has a saddle point (u^*, v^*), and the players u and v have a finite number of strategies given by

$$U = \{u_1, u_2, \ldots, u_{N_u}\} \tag{8}$$

$$V = \{v_1, v_2, \ldots, v_{N_v}\} \tag{9}$$

where N_u and N_v denote the number of strategies of u and v, respectively. Then, (F, U, V) characterizes a matrix game, of which the solution is determined from the security strategies of the two players. The security strategy of u, denoted as u^s, is the strategy that gives the minimum worst-case payoff for u (Ref. 10):

$$\max_j F(u^s, v_j) \le \max_j F(u_i, v_j), \qquad i = 1, \ldots, N_u \tag{10}$$

Similarly, the security strategy of v, denoted as v^s, satisfies

$$\min_i F(u_i, v^s) \ge \min_i F(u_i, v_j), \qquad j = 1, \ldots, N_v \tag{11}$$

Now we interpret a static matrix game in the context of coevolution. First, introduce new variables X_i and Y_j to denote individuals representing the strategies u_i and v_j, respectively. Group X is then defined as the collection of all X_i and group Y the collection of all Y_j. The score of the match between X_i and Y_j is defined as the value of $F(u_i, v_j)$. Because the solution of the zero-sum game is determined from the security strategy, each group's fitness evaluation should also be based on its security strategy; i.e., the fitness of each individual is determined by the worst score among all the match scores the individual obtains. Thus,

$$\text{fitness of } X_i = \max_j F(X_i, Y_j) \tag{12}$$

$$\text{fitness of } Y_j = -\min_i F(X_i, Y_j) \tag{13}$$

Selection and variation of each group can be accomplished by any of the schemes used in single-group evolutionary algorithms such as evolutionary programming, evolution strategy, and genetic algorithms. For the numerical examples presented here, we employed the algorithm of evolution strategy, specifically, the (μ, λ)-method described in Ref. 11. Note that we only need to evaluate $f(\boldsymbol{x})$, $g(\boldsymbol{x})$, and $h(\boldsymbol{x})$ for N_u times, as in other single-group evolutionary methods. For an individual X_i, the value of $L_A(X_i, Y_j)$ for any Y_j is easily computed by a simple calculation of the penalty terms.

Numerical Example and Results

The design variables $\boldsymbol{x}$ are the cross-sectional areas of the truss bar elements, and the objective function is the total weight, which can be expressed as

$$J = \sum_{i=1}^{N} \rho_i A_i l_i \tag{14}$$

where N is the number of bar elements, and ρ_i, A_i, l_i denote the density, cross-sectional area, and length of ith element, respectively. The constraints are the allowable stress for each bar element specified in both tension and compression as follows:

$$\sigma_l \le \sigma_i^{(j)} \le \sigma_u \tag{15}$$

where $\sigma_i^{(j)}$ denotes the stress in member i under load condition j, σ_u is the allowable tensile stress, and σ_l denotes the allowable compressive stress. Thin-walled tubular members are used for truss bar elements with a maximum mean radius of 2 in. Other constraints include displacement limits at specified nodes:

$$\delta_l \le \delta_{i,k} \le \delta_u \tag{16}$$

where $\delta_{i,k}$ denotes the deflection of node i along the kth axis, and δ_l and δ_u denote the displacement limits in each direction. There are

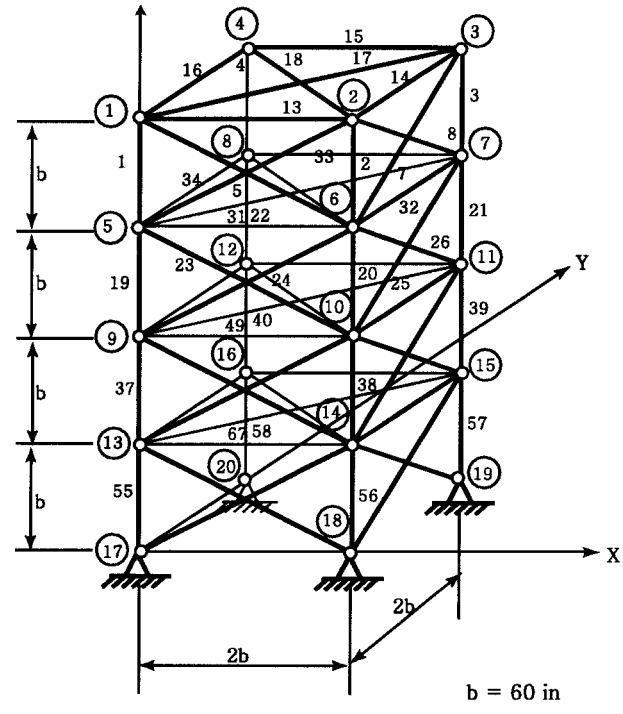

Fig. 1 Seventy-two-bar truss structure.

Table 1 Optimized weights of the 72-bar truss

General number	Weight, lb			
	Best	Worst	Median	Mean
100	422.47	459.10	430.94	436.30
200	385.21	450.90	408.65	412.70
300	383.50	448.91	402.04	407.28
400	383.50	442.63	401.91	404.81
500	383.30	438.63	398.81	402.11
600	381.15	418.94	394.03	394.71
700	381.02	403.67	387.60	390.74
800	381.02	401.31	383.91	388.27
900	380.75	395.04	382.48	385.68
1000	380.26	394.99	381.98	383.99
1500	379.83	384.64	380.49	381.06
2000	379.71	382.31	380.06	380.27

Table 2 Optimal areas of the 72-bar truss

Variable	Area, in.^{2}		
	Reference 8	Best solution	Worst solution
1	0.1571	0.1565	0.1492
2	0.5356	0.5467	0.5743
3	0.4099	0.4008	0.3890
4	0.5690	0.5785	0.5416
5	0.5067	0.5198	0.5325
6	0.5200	0.5163	0.5135
7	0.1000	0.1000	0.1000
8	0.1000	0.1006	0.2260
9	1.2800	1.3005	1.0878
10	0.5148	0.5070	0.5145
11	0.1000	0.1001	0.1001
12	0.1000	0.1002	0.1001
13	1.8970	1.8726	1.9125
14	0.5158	0.5153	0.5218
15	0.1000	0.1002	0.1002
16	0.1000	0.1001	0.1004
Weight, lb	379.66	379.71	382.31

also side constraints on the design variables so that the bar elements will not be designed too thin:

$$A_i \geq A_{\min} \tag{17}$$

where $A_{\min}$ denotes the minimum area of each bar element.

Figure 1 shows the 72-bar truss structure studied in Refs. 7 and 8. A total of 16 design variables are used to represent the areas of bar elements:

$$x_1 = A_1 = \cdots = A_4, \qquad x_2 = A_5 = \cdots = A_{12}$$

$$x_3 = A_{13} = \cdots = A_{16}, \qquad x_4 = A_{17} = A_{18}$$

$$x_5 = A_{19} = \cdots = A_{22}, \qquad x_6 = A_{23} = \cdots = A_{30}$$

$$x_7 = A_{31} = \cdots = A_{34}, \qquad x_8 = A_{35} = A_{36}$$

$$x_9 = A_{37} = \cdots = A_{40}, \qquad x_{10} = A_{41} = \cdots = A_{48}$$

$$x_{11} = A_{49} = \cdots = A_{52}, \qquad x_{12} = A_{53} = A_{54}$$

$$x_{13} = A_{55} = \cdots = A_{58}, \qquad x_{14} = A_{59} = \cdots = A_{66}$$

$$x_{15} = A_{67} = \cdots = A_{70}, \qquad x_{16} = A_{71} = A_{72}$$

All truss members are aluminum, and the Young's modulus and the specific mass of all bar elements are taken as $E = 10^7$ psi and $\rho = 0.1$ lb/in.^{3}. The allowable stresses in tension and compression for the bar elements are specified as $\pm 25{,}000$ lb/in.^{2}, and the minimum cross-sectional area is taken as 0.1 in.^{2} for each bar element. In addition to the stress and minimum area constraints, displacement limits of ± 0.25 in. are imposed on nodes 1–4 in the x and z directions under the two load conditions:

$$\text{Load condition 1:} \quad P_x^{(1)} = P_y^{(1)} = 5000 \text{ lb}, \qquad P_z^{(1)} = -5000 \text{ lb}$$

$$\text{Load condition 2:} \quad P_z^{(1)} = P_z^{(2)} = P_z^{(3)} = P_z^{(4)} = -5000 \text{ lb}$$

where the superscript denotes the bar to which the external load is applied. Other load components are all assumed zero.

The parent and offspring population sizes are chosen as 4 and 20, respectively. The evolution process of 2000 generations is simulated for 10 iterations. Computation time is about 8.2 s for each generation on a 266-MHz Pentium PC. The optimized weights are summarized in Table 1. Note that the coevolution algorithm finds the solution area within 100 generations. The optimal weight of Ref. 8 is 379.66 lb, which is 0.05 lb smaller than the best result of coevolution of 2000 generations, as shown in Table 2.

Conclusion

A coevolution method for solving a large class of optimization problems such as those encountered in structural optimization is introduced in this Note. This new method solves static zero-sum games or saddle-point problems by an artificial evolution of two groups with opposite objectives. The 72-bar truss problem is used as an example model to verify the proposed coevolution method. Numerical results show that the coevolution method can achieve the global solution with an accuracy comparable to that of conventional nonlinear programming techniques. Furthermore, the coevolution method is robust to initial conditions, producing consistent solutions.

References

[1] Lin, C.-Y., and Hajela, J., "Genetic Search Strategies in Large Scale Optimization," *Proceedings of the AIAA/ASME/ASCE/AHS/ASC 34th Structures, Structural Dynamics, and Materials Conference*, AIAA, Washington, DC, 1993, pp. 2437–2447.

[2] Dhingra, A. K., and Bennage, W. A., "Discrete and Continuous Variable Structural Optimization Using Tabu Search," *Engineering Optimization,* Vol. 24, No. 3, 1995, pp. 177–196.

[3] Rao, S. S., and Chen, L., "Generalized Hybrid Method for Fuzzy Multiobjective Optimization of Engineering Systems," *AIAA Journal*, Vol. 34, No. 8, 1996, pp. 1709–1717.

[4] Rajeev, S., and Krishnamoorthy, C. S., "Genetic Algorithm-Based Methodologies for Design Optimization of Trusses," *Journal of Structural Engineering*, Vol. 123, No. 3, 1997, pp. 350–358.

[5] Michalewicz, Z., and Schoenaur, M., "Evolutionary Algorithms for Constrained Parameter Optimization Problems," *Evolutionary Computation,* Vol. 4, No. 1, 1996, pp. 1–32.

[6] Tahk, M. J., "Co-Evolution for Engineering Optimization Problems: Minimax Design and Constrained Optimization (Special Lecture)," *Proceeding of the JSASS 36th Aircraft Symposium*, Japan Society of Aeronautical and Space Sciences, Yokosuka, Japan, 1998, pp. 679–685.

[7] Fleury, C., and Schmit, L. A., "Dual Methods and Approximation Concepts in Structural Synthesis," NASA CR-3226, Dec. 1980.

[8] Haftka, R. T., Gürdal, Z., and Kamat, M. P., *Elements of Structural Optimization,* Kluwer, Dordrecht, The Netherlands, 1990, Chap. 6.

[9] Bazaraa, M. S., Sherali, H. D., and Shetty, C. M., *Nonlinear Programming: Theory and Algorithms,* 2nd ed., Wiley, New York, 1993, Chap. 9.

[10] Basar, T., and Olsder, G. J., *Dynamic Noncooperative Game Theory,* Academic, London, 1982, Chap. 2.

[11] Bäck, T., *Evolutionary Algorithms in Theory and Practice,* Oxford Univ. Press, New York, 1996, Chap. 2.

A. Chattopadhyay
Associate Editor